Substitution of larger Dy^{3+} ions in Ni-Zn-Fe-O nanoferrites synthesized by sol-gel auto-combustion technique.

S. S. Kammar

Department of Physics, HKE's A. V. Patil Degree College, Aland, Dist. Kalburgi (KA) India.

Abstract:

Sol-gel auto-combustion technique was employed to produce the rare-earth (RE) Dy^{3+} doped Ni-Zn-Fe-O nano-crystalline powders. Newly prepared powders were sintered at 800^0C for 6 hrs. Powder X-ray diffraction technique (XRD) was used to estimate the structure of the samples and related structural parameters. XRD patterns suggests that the single-phase cubic spinel structure of the samples with no trace of any impurity phase. Substitution of larger Dy^{3+} ions in Ni-Zn crystal lattice increases the lattice constant from 8.3663 to 8.3811 Å. XRD data was used to estimate the other structural parameters like X-ray density (d_X), porosity (P), specific surface area (S), hopping lengths (L_A, L_B) and other allied parameters tetrahedral and octahedral bond length (d_{Ax}, d_{Bx}), tetrahedral edge, octahedral edge (shared and unshared) ($d_{AXE,}$ $d_{BXE,}$ and d_{BXEU}). Larger Dy^{3+} ions substitution varies the structural parameters of Ni-Zn spinel ferrites.

Keywords: Sol-gel technique, rare earth ions, lattice constant, hopping lengths.

Introduction:

Wide range of potential applications in high density magnetic recording media, memory chips, biomedical and microwave applications, magnetic fluids, core transformers etc. gaining the attention of scientists and technologists towards magnetic nanoparticles [1-4]. In the recent years, ferrites with spinel structure have been extensively investigated by the researchers by considering the importance in basic and applied research [5-6]. Rare earth (RE) doped spinel ferrites have attracted much attention within the scientists and materials researchers due to their unusual properties like infrared emission, catalytic activities, photoelectric emission and magnetic interactions [7-8]. It is known that the magnetic interaction of the ferromagnetic oxides is largely governed by the coupling of spins of the 3d electrons (Fe-Fe interactions). Introduction of RE ions in the spinel lattice introduces the ad-4f coupling (RE-Fe interactions) which can lead to small changes in the magnetization and Curie point [9].

Several researchers have been investigated the spinel ferrites by introducing the RE ions. Spinel ferrites having general chemical formula AB_2O_4, where, A-represents the divalent metal ion (Ex. Mn^{2+}, Ni^{2+}, Zn^{2+}, Co^{2+}, Cu^{2+} etc.) and B represents the trivalent metal ion specially Fe^{3+} ions. Larger RE ions, generally, replaces the smaller Fe^{3+} ions at octahedral – B site. Due to larger ionic radii, even in small amount, introduction of Dy^{3+} ions in Ni-Zn ferrites greatly affects the structural, electrical and magnetic properties. In the present paper, structural properties of Dy^{3+} doped Ni-Zn ferrites have been discussed.

Experimental

Sol-gel auto-combustion technique have been adopted to prepare the Dy^{3+} doped Ni-Zn ferrites having general chemical formula as $Ni_{0.7}Zn_{0.3}Dy_xFe_{2-x}O_4$ (x = 0.0, 0.015, 0.03). This method is adopted because homogeneous mixing of the chemical constituents on the atomic scale and better sinter ability will be achieved. AR grade (99%n pure) Nickel nitrate ($Ni(NO_3)_2.6H_2O$), Zinc nitrate ($Zn(NO_3)_2.6H_2O$), Dysprosium nitrate ($Dy(NO_3)_3.9H_2O$) and citric acid ($C_6H_8O_7.H_2O$) were taken with their weight proportion in the composition for the synthesis of $Ni_{0.7}Zn_{0.3}Dy_xFe_{2-x}O_4$ (x = 0.0, 0.015, 0.03). Reaction procedure was carried out in air atmosphere without protection of inert gases. Citric acid was used as chelating agent and was taken in 1:3 ratio with metal nitrates. All the metal nitrates and citric acid was dissolved in sufficient amount of glass distilled water to get a clear solution. pH of the solution was maintained at neutral (≅ 7) value by adding the liquid ammonia dropwise. Whole solution in beaker was stirred at half an hour and then kept on magnetic stirrer with hot plate. The solution was heated at constant temperature of 90^0C with constant stirring. After couple of hours, the solution becomes viscous and transformed in to sol and after some time converted into dried gel. When ignited at any point of the gel, the dried gel burnt in a self -propagating combustion manner until all gels were completely burnt out to form a fluffy loose powder. The auto-ignition of gel was carried out in glass beaker upon a hot plate. The auto-combustion was completed within a minute, yielding the brown – coloured ashes termed as a precursor. The as prepared powders then sintered at 800 ^{0}C for six hours. Structure of the samples and other structural parameters were investigated by using powder X-ray diffraction data. The XRD patterns of all the samples were recorded at room temperature within the 2θ range of 20^0 to 70^0. Phillips X-ray diffractometer (Model 3710) was used to record the XRD patterns by using Cu-K_α radiation having wavelength λ = 1.5406 Å. Scanning rate was maintained at 2^0 per minute. The obtained XRD data was used to study the structural parameters.

Results and Discussion

Room temperature powder X-ray diffraction patterns of $Ni_{0.7}Zn_{0.3}Dy_xFe_{2-x}O_4$ (x = 0.0, 0.015, 0.03) nano-ferrites are shown in Fig. 1. All the XRD lines are well indexed for the planes (220), (311), (222), (400), (422), (333) and (440) nearly at an glancing angles 30.22^0, 35.59^0, 37.21^0, 43.25^0, 53.64^0, 57.17^0 and 62.78^0. All the peaks are observed to be brad and no any impurity phase is observed in the XRD lines. This implies that the Dy^{3+} ions are successfully incorporated in the Ni-Zn crystal lattice.

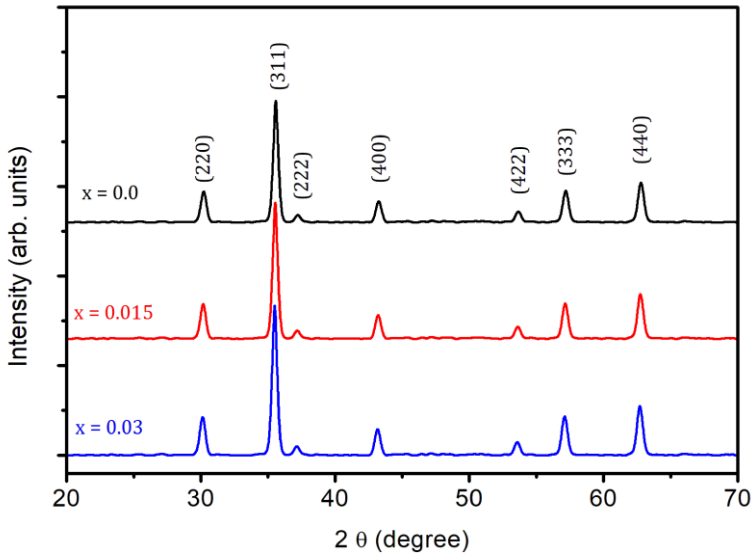

Fig. 1: X-ray diffraction lines of $Ni_{0.7}Zn_{0.3}Dy_xFe_{2-x}O_4$ nano-ferrites.

A keen observation of XRD patterns shows that the peak positions are slightly shifted towards lower angle positions which in turn enhances the lattice lengths. The lattice parameter 'a' for all the cubic structured samples was evaluated by using the Bragg's law as a function of Dy^{3+} content [10].

$$a = d\left(h^2 + k^2 + l^2\right)^{1/2} \qquad (1)$$

Where, a – is lattice parameter, d – is inter-planner spacings and (hkl) are the miller indices. For every indexed peak lattice parameter was computed and finally the average was taken. The variation of lattice parameter 'a' with Dy^{3+} substitution is depicted in Fig. 2. It can be seen that the lattice parameter 'a' increases from 8.3663 to 8.3811 Å with the addition of Dy^{3+} ions. This increase may be due to the substitution of smaller Fe^{3+} ions (0.65 Å) by larger Dy^{3+} (1.05 Å).

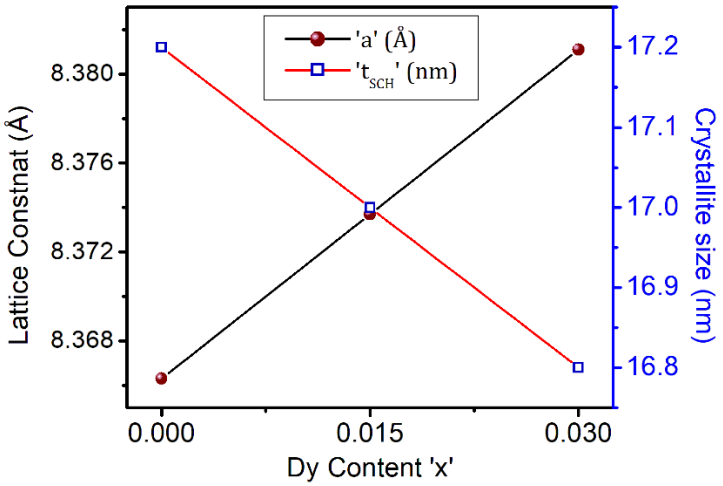

Fig. 2: Variation of lattice parameter (a) and crystallite size (t) for $Ni_{0.7}Zn_{0.3}Dy_xFe_{2-x}O_4$ nano-ferrites.

Average crystallite size (t_{xrd}) was estimated by using well – known Scherrer equation given below [11];

$$t_{XRD} = \frac{0.9\lambda}{\beta \mathrm{Cos}\left(\theta_B\right)} \qquad (2)$$

Where, λ is incident XRD wavelength (≅1.5406 Å), β - full width at it its half maximum (FWHM) and θ_B is the Bragg's position. As depicted in Fig. 2, crystallite size (t_{XRD}) decreases from 17.2 to 16.8 nm with the increasing percentage of Dy^{3+} ions. Other crystallographic parameters like X-ray density, porosity and specific surface area were estimated by using XRD data. Bulk density of all the sample was estimated by using simple mass-volume relation and the values are obtained in the range 4.844 to 4.746 gm/cc. X-ray density of all the samples was estimated by using the relation [12];

$$d_X = \frac{8M}{Na^3} \qquad (3)$$

Where, 8 is the number of molecules per unit cell for cubic structure, M is the molecular weight of the composition, N is the Avagadro's number and 'a' is the lattice parameter. It can be seen from Fig. 3 that the X-ray density increases from 5.363 to 5.406 gm/cc with the addition of Dy^{3+} ions in Ni-Zn lattice. Both molecular weight and unit cell volume of the samples increases with the addition of Dy^{3+} ions, but the increment in molecular weight is more than that of cell increment in unit cell volume. Therefore, the X-ray density increases with the addition of Dy^{3+} ions in Ni-Zn lattice.

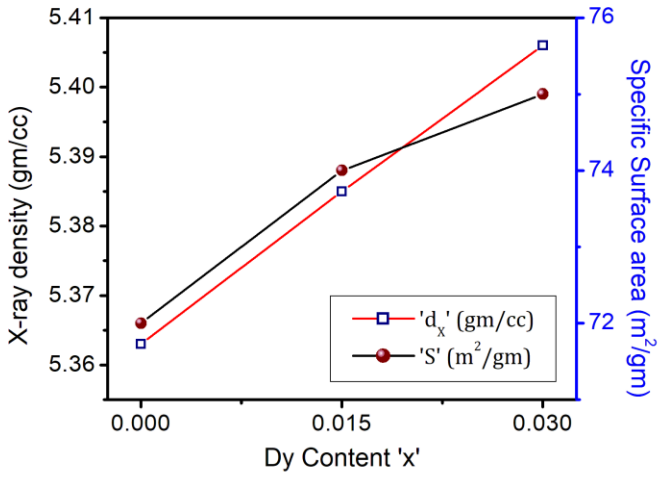

Fig. 3: Variation of X-ray density (d_X) and specific surface area (S) for $Ni_{0.7}Zn_{0.3}Dy_xFe_{2-x}O_4$ nano-ferrites.

Porosity of the samples in percentage (P) was estimated by using the following relation [12];

$$P(\%) = \left(\frac{d_X - d_B}{d_X}\right) \times 100 \qquad (4)$$

Where, d_X is X-ray density and d_B is Bulk density. Percentage porosity increases from 9.68 to 12.22 % with substitution of Fe^{3+} ions by Dy^{3+} ions. Specific surface area was estimated by using the relation given below [13];

$$S = \frac{6000}{t_{XRD} \times d_B} \qquad (5)$$

Where, t_{XRD} is the crystallite size and 'd_B' is the bulk density. Fig. 3 shows the variation of specific surface area 'S' with Dy^{3+} addition. It can be seen that the specific surface area increases from 72 to 75 m^2/gm with the increasing percentage of Dy^{3+} ions.

Hopping lengths 'L_A', 'L_B' and allied parameters such as tetrahedral and octahedral bond lengths (d_{AX} and d_{BX}) tetrahedral edge, shared and unshared octahedral edge (d_{AXE}, d_{BXE}, and d_{BXEU}) were calculated by using following relations [14];

$$L_A = a\left(\frac{3}{4}\right)^{1/2} \quad (6)$$

$$L_B = a\left(\frac{2}{4}\right)^{1/2} \quad (7)$$

$$d_{AX} = a\sqrt{3}\left(u - 1/4\right) \quad (8)$$

$$d_{BX} = a\left[3u^2 - (11/4)u + 43/64\right]^{1/2} \quad (9)$$

$$d_{AXE} = a\sqrt{2}\left(2u - 1/2\right) \quad (10)$$

$$d_{BXE} = a\sqrt{2}\left(1 - 2u\right) \quad (11)$$

$$d_{BXEU} = a\left[4u^2 - 3u + (11/16)\right]^{1/2} \quad (12)$$

Fig. 4 shows the variation of hopping lengths 'L_A' and L_B' with Dy^{3+} substitution. Both 'L_A' and L_B' increases from 3.6227 to 3.6291 Å and 2.9579 to 2.9632 Å respectively with the addition of Dy^{3+} ions in Ni-Zn crystal lattice. The variation in hopping lengths is consistent with the variation in lattice parameter.

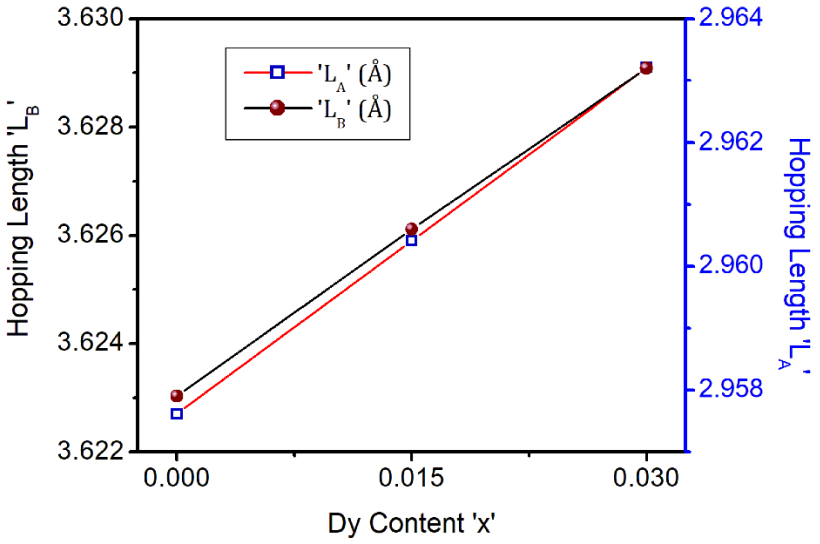

Fig. 4: Variation of hopping lengths (L_A and L_B) for $Ni_{0.7}Zn_{0.3}Dy_xFe_{2-x}O_4$ nano-ferrites.

Table 1: Allied parameters of $Ni_{0.7}Zn_{0.3}Dy_xFe_{2-x}O_4$.

'x'	'd_{AX}' (Å)	'd_{BX}' (Å)	'd_{AXE}' (Å)	'd_{BAX}' (Å)	'd_{BXEU}' (Å)
0.0	1.9534	2.0129	3.1898	2.7260	2.9625
0.015	1.9900	1.9965	3.2496	2.6715	2.9676
0.03	2.0142	1.9867	3.2891	2.6372	2.9721

Table 1 represents the values of allied parameters such as tetrahedral and octahedral bond lengths (d_{AX} and d_{BX}) tetrahedral edge, shared and unshared octahedral edge (d_{AXE}, d_{BXE}, and d_{BXEU}) calculated by using the relations (8-12). The addition of Dy^{3+} ions enhances the tetrahedral bond length (d_{AX}) from

1.9534 to 2.0142 Å while as reduces the octahedral bond length (d_{BX}) from 2.0129 to 1.9867 Å. Tetrahedral edge (d_{AXE}) increases from 3.1898 to 3.2891 Å, shared octahedral edge (d_{BAX}) decreases from 2.7260 to 2.6372 Å and unshared octahedral edge (d_{BXEU}) increases from 2.9625 to 2.9721 Å with the addition of Dy^{3+} ions in Ni-Zn crystal lattice. This variation of allied parameters is strongly related to the variation in lattice parameter. As discussed earlier in this paper, in the present case, larger Dy^{3+} ions replaces the smaller Fe^{3+} ions. The difference in ionic radii of both the atoms is reflected in the values of lattice parameter and also in the values of all allied parameters.

Conclusions

Dy^{3+} substituted Ni-Zn-Fe-O nano-ferrites were successfully obtained by using sol-gel auto-combustion technique. Incorporation of larger Dy^{3+} ions in Ni-Zn crystal lattice increases the lattice parameter from 8.3663 to 8.3811 Å while as decreases the crystallite size from 17.2 to 16.8 nm. X-ray density, porosity and specific surface area increases with the addition of Dy^{3+} ions. Both hopping lengths shows increasing behaviour which is consistent with the variation of lattice constant. Allied parameters are related with the variation in lattice constant.

References

[1] A. B. Kadam, V. K. Mande, S. B. Kadam, R. H. Kadam, S. E. Shirsath, R. B. Borade; Influence of gadolinium (Gd^{3+}) ion substitution on structural, magnetic and electrical properties of cobalt ferrites; J. Alloys. Comp. 840 (2020) 155669.

[2] J. Hu, Y. Ma, X. Kan, C. Liu, X. Zhang, R. Rao, M. Wang, G. Zheng; Investigations of co-substitution on the structural and magnetic properties of Ni-Zn spinel ferrite; J. Magn. Magn. Mater. 513 (2020) 167200

[3] V. D. More, S. R. Kadam, S. B. Shelke, P. D. Gaikwad, R. H. Kadam, S. T. Alone; Modified structural and magnetic properties of Ni-Mn-Zn ferrite nanoparticles doped with Ce^{3+} ions; Biointer. Res. Appl. Chem. 12 (2022) 5021-5030.

[4] V. D. More, S. S. Kadam, S. R. Kadam, S. R. Wadgane, R. H. Kadam, S. T. Alone; Complete micro-structural analysis and elastic properties of Sm^{3+} doped Ni-Mn-Zn mixed spinel ferrite nanoparticles; 400 (2021) 2100115.

[5] S. Ikram, J. Jacob, M. I. Arshad, K. Mahmood, A. Ali, N. Sabir, N. Amin, S. Hussain; Tailoring the structural, magnetic and dielectric properties of Ni-Zn $CdFe_2O_4$ spinel ferrites by the substitution of lanthanum ions; Ceram. Inter. 45 (2019) 3563-3569.

[6] V. Chaudhari, R. H. Kadam, M. L. Mane, S. E. Shirsath, A. B. Kadam, D. R. Mane; Effect of La^{3+} impurity on magnetic and electrical properties of Co-Cu-Cr-Fe nanoparticles; J. Nanosci. Nanotechn. 15 (2015) 4268-4275.

[7] M. Houshiar, L. Jamilpanah; Effect of Cu dopant on the structural, magnetic and electrical properties of Ni-Zn ferrites; Mater. Res. Bull. 98 (2018) 213-218.

[8] M. N. Akthar, M. A. Khan; Effect of rare earth doping on the structural and magnetic features of nanocrystalline spinel ferrites prepared via sol-gel route; J. Magn. Magn. Mater. 460 (2018) 268-277.

[9] M. Yousuf, S. Nazir, M. Akbar, M. N. Akthar, A. Noor, E. Hu, M. A. K. Yousuf Shaikh, Y. Lu; Structural, magnetic and electrical evaluations of rare earth Gd^{3+} doped in mixed Co-Mn spinel ferrites; Ceram. Inter. 48 (2022) 578-586.

[10] K. R. Desai, S. T. Alone, S. R. Wadgane, S. E. Shirsath, K. M. Batoo, A. Imran, E. H. Raslan, M. Hadi, M. F. Ijaz, R. H. Kadam; X-ray diffraction based Williamson-Hall analysis and Rietveld refinement for strain mechanism in Mg-Mn co-substituted $CdFe_2O_4$ nanoparticles; Physica B: Cond. Matter. 614 (2021) 413054.

[11] Z. Karimi, Y. Mohammadifar, H. Shokrollahi, Sh. Khamenesh Asl., Gh. Yousefi, L. Karimi; Magnetic and structural properties of nano-sized Dy-doped cobalt ferrite synthesized by co-precipitation; J. Magn. Magn. Mater. 361 (2014) 150-156.

[12] D. V. Phugate, R. B. Borade, S. B. Kadam, L. A. Dhale, R. H. Kadam, S. E. Shirsath, A. B. Kadam; Effect of Ho^{3+} ion doping on thermal, structural, and morphological properties of Co-Ni ferrite synthesized by sol-gel method; J. Supercond. Nov. Magn. 33 (2020) 3545-3554.

[13] M. Junaid, M. A. Khan, F. Iqbal, G. Murtaza, M. N. Akthar, M. Ahmad, I. Shakir, M. F. Warsi; J. Magn. Magn. Mater. 419 (2016) 338-344

[14] M. Hashim, A. Ahmed, S. A. Ali, S. E. Shirsath, M. M. Ismail, R. Kumar, S. Kumar, S. S. Meena, D. Ravinder; J. Alloys. Comp. 834 (2020) 155089.